FERMILAB-PUB-05-087-E

Measurement of the $t\bar{t}$ Production Cross Section in $p\bar{p}$ Collisions at $\sqrt{s} = 1.96$ TeV using Lepton + Jets Events with Lifetime b-tagging

arXiv:hep-ex/0504058 v1 28 Apr 2005

V.M. Abazov,[35] B. Abbott,[72] M. Abolins,[63] B.S. Acharya,[29] M. Adams,[50] T. Adams,[48] M. Agelou,[18] J.-L. Agram,[19] S.H. Ahn,[31] M. Ahsan,[57] G.D. Alexeev,[35] G. Alkhazov,[39] A. Alton,[62] G. Alverson,[61] G.A. Alves,[2] M. Anastasoaie,[34] T. Andeen,[52] S. Anderson,[44] B. Andrieu,[17] Y. Arnoud,[14] A. Askew,[48] B. Åsman,[40] A.C.S. Assis Jesus,[3] O. Atramentov,[55] C. Autermann,[21] C. Avila,[8] F. Badaud,[13] A. Baden,[59] B. Baldin,[49] P.W. Balm,[33] S. Banerjee,[29] E. Barberis,[61] P. Bargassa,[76] P. Baringer,[56] C. Barnes,[42] J. Barreto,[2] J.F. Bartlett,[49] U. Bassler,[17] D. Bauer,[53] A. Bean,[56] S. Beauceron,[17] M. Begel,[68] A. Bellavance,[65] S.B. Beri,[27] G. Bernardi,[17] R. Bernhard,[49,*] I. Bertram,[41] M. Besançon,[18] R. Beuselinck,[42] V.A. Bezzubov,[38] P.C. Bhat,[49] V. Bhatnagar,[27] M. Binder,[25] C. Biscarat,[41] K.M. Black,[60] I. Blackler,[42] G. Blazey,[51] F. Blekman,[33] S. Blessing,[48] D. Bloch,[19] U. Blumenschein,[23] A. Boehnlein,[49] O. Boeriu,[54] T.A. Bolton,[57] F. Borcherding,[49] G. Borissov,[41] K. Bos,[33] T. Bose,[67] A. Brandt,[74] R. Brock,[63] G. Brooijmans,[67] A. Bross,[49] N.J. Buchanan,[48] D. Buchholz,[52] M. Buehler,[50] V. Buescher,[23] S. Burdin,[49] T.H. Burnett,[78] E. Busato,[17] C.P. Buszello,[42] J.M. Butler,[60] J. Cammin,[68] S. Caron,[33] W. Carvalho,[3] B.C.K. Casey,[73] N.M. Cason,[54] H. Castilla-Valdez,[32] S. Chakrabarti,[29] D. Chakraborty,[51] K.M. Chan,[68] A. Chandra,[29] D. Chapin,[73] F. Charles,[19] E. Cheu,[44] D.K. Cho,[60] S. Choi,[47] B. Choudhary,[28] T. Christiansen,[25] L. Christofek,[56] D. Claes,[65] B. Clément,[19] C. Clément,[40] Y. Coadou,[5] M. Cooke,[76] W.E. Cooper,[49] D. Coppage,[56] M. Corcoran,[76] A. Cothenet,[15] M.-C. Cousinou,[15] B. Cox,[43] S. Crépé-Renaudin,[14] D. Cutts,[73] H. da Motta,[2] B. Davies,[41] G. Davies,[42] G.A. Davis,[52] K. De,[74] P. de Jong,[33] S.J. de Jong,[34] E. De La Cruz-Burelo,[32] C. De Oliveira Martins,[3] S. Dean,[43] J.D. Degenhardt,[62] F. Déliot,[18] M. Demarteau,[49] R. Demina,[68] P. Demine,[18] D. Denisov,[49] S.P. Denisov,[38] S. Desai,[69] H.T. Diehl,[49] M. Diesburg,[49] M. Doidge,[41] H. Dong,[69] S. Doulas,[61] L.V. Dudko,[37] L. Duflot,[16] S.R. Dugad,[29] A. Duperrin,[15] J. Dyer,[63] A. Dyshkant,[51] M. Eads,[51] D. Edmunds,[63] T. Edwards,[43] J. Ellison,[47] J. Elmsheuser,[25] V.D. Elvira,[49] S. Eno,[59] P. Ermolov,[37] O.V. Eroshin,[38] J. Estrada,[49] H. Evans,[67] A. Evdokimov,[36] V.N. Evdokimov,[38] J. Fast,[49] S.N. Fatakia,[60] L. Feligioni,[60] A.V. Ferapontov,[38] T. Ferbel,[68] F. Fiedler,[25] F. Filthaut,[34] W. Fisher,[66] H.E. Fisk,[49] I. Fleck,[23] M. Fortner,[51] H. Fox,[23] S. Fu,[49] S. Fuess,[49] T. Gadfort,[78] C.F. Galea,[34] E. Gallas,[49] E. Galyaev,[54] C. Garcia,[68] A. Garcia-Bellido,[78] J. Gardner,[56] V. Gavrilov,[36] P. Gay,[13] D. Gelé,[19] R. Gelhaus,[47] K. Genser,[49] C.E. Gerber,[50] Y. Gershtein,[48] D. Gillberg,[5] G. Ginther,[68] T. Golling,[22] N. Gollub,[40] B. Gómez,[8] K. Gounder,[49] A. Goussiou,[54] P.D. Grannis,[69] S. Greder,[3] H. Greenlee,[49] Z.D. Greenwood,[58] E.M. Gregores,[4] Ph. Gris,[13] J.-F. Grivaz,[16] L. Groer,[67] S. Grünendahl,[49] M.W. Grünewald,[30] S.N. Gurzhiev,[38] G. Gutierrez,[49] P. Gutierrez,[72] A. Haas,[67] N.J. Hadley,[59] S. Hagopian,[48] I. Hall,[72] R.E. Hall,[46] C. Han,[62] L. Han,[7] K. Hanagaki,[49] K. Harder,[57] A. Harel,[26] R. Harrington,[61] J.M. Hauptman,[55] R. Hauser,[63] J. Hays,[52] T. Hebbeker,[21] D. Hedin,[51] J.M. Heinmiller,[50] A.P. Heinson,[47] U. Heintz,[60] C. Hensel,[56] G. Hesketh,[61] M.D. Hildreth,[54] R. Hirosky,[77] J.D. Hobbs,[69] B. Hoeneisen,[12] M. Hohlfeld,[24] S.J. Hong,[31] R. Hooper,[73] P. Houben,[33] Y. Hu,[69] J. Huang,[53] V. Hynek,[9] I. Iashvili,[47] R. Illingworth,[49] A.S. Ito,[49] S. Jabeen,[56] M. Jaffré,[16] S. Jain,[72] V. Jain,[70] K. Jakobs,[23] A. Jenkins,[42] R. Jesik,[42] K. Johns,[44] M. Johnson,[49] A. Jonckheere,[49] P. Jonsson,[42] A. Juste,[49] D. Käfer,[21] S. Kahn,[70] E. Kajfasz,[15] A.M. Kalinin,[35] J. Kalk,[63] D. Karmanov,[37] J. Kasper,[60] D. Kau,[48] R. Kaur,[27] R. Kehoe,[75] S. Kermiche,[15] S. Kesisoglou,[73] A. Khanov,[68] A. Kharchilava,[54] Y.M. Kharzheev,[35] H. Kim,[74] T.J. Kim,[31] B. Klima,[49] J.M. Kohli,[27] M. Kopal,[72] V.M. Korablev,[38] J. Kotcher,[70] B. Kothari,[67] A. Koubarovsky,[37] A.V. Kozelov,[38] J. Kozminski,[63] A. Kryemadhi,[77] S. Krzywdzinski,[49] Y. Kulik,[49] A. Kumar,[28] S. Kunori,[59] A. Kupco,[11] T. Kurča,[20] J. Kvita,[9] S. Lager,[40] N. Lahrichi,[18] G. Landsberg,[73] J. Lazoflores,[48] A.-C. Le Bihan,[19] P. Lebrun,[20] W.M. Lee,[48] A. Leflat,[37] F. Lehner,[49,*] C. Leonidopoulos,[67] J. Leveque,[44] P. Lewis,[42] J. Li,[74] Q.Z. Li,[49] J.G.R. Lima,[51] D. Lincoln,[49] S.L. Linn,[48] J. Linnemann,[63] V.V. Lipaev,[38] R. Lipton,[49] L. Lobo,[42] A. Lobodenko,[39] M. Lokajicek,[11] A. Lounis,[19] P. Love,[41] H.J. Lubatti,[78] L. Lueking,[49] M. Lynker,[54] A.L. Lyon,[49] A.K.A. Maciel,[51] R.J. Madaras,[45] P. Mättig,[26] C. Magass,[21] A. Magerkurth,[62] A.-M. Magnan,[14] N. Makovec,[16] P.K. Mal,[29] H.B. Malbouisson,[3] S. Malik,[58] V.L. Malyshev,[35] H.S. Mao,[6] Y. Maravin,[49] M. Martens,[49] S.E.K. Mattingly,[73] A.A. Mayorov,[38] R. McCarthy,[69] R. McCroskey,[44] D. Meder,[24] A. Melnitchouk,[64] A. Mendes,[15] M. Merkin,[37] K.W. Merritt,[49] A. Meyer,[21] J. Meyer,[22] M. Michaut,[18] H. Miettinen,[76] J. Mitrevski,[67] J. Molina,[3] N.K. Mondal,[29] R.W. Moore,[5] G.S. Muanza,[20] M. Mulders,[49] Y.D. Mutaf,[69] E. Nagy,[15] M. Narain,[60] N.A. Naumann,[34] H.A. Neal,[62] J.P. Negret,[8] S. Nelson,[48] P. Neustroev,[39]

C. Noeding,[23] A. Nomerotski,[49] S.F. Novaes,[4] T. Nunnemann,[25] E. Nurse,[43] V. O'Dell,[49] D.C. O'Neil,[5] V. Oguri,[3] N. Oliveira,[3] N. Oshima,[49] G.J. Otero y Garzón,[50] P. Padley,[76] N. Parashar,[58] S.K. Park,[31] J. Parsons,[67] R. Partridge,[73] N. Parua,[69] A. Patwa,[70] G. Pawloski,[76] P.M. Perea,[47] E. Perez,[18] P. Pétroff,[16] M. Petteni,[42] R. Piegaia,[1] M.-A. Pleier,[68] P.L.M. Podesta-Lerma,[32] V.M. Podstavkov,[49] Y. Pogorelov,[54] A. Pompoš,[72] B.G. Pope,[63] W.L. Prado da Silva,[3] H.B. Prosper,[48] S. Protopopescu,[70] J. Qian,[62] A. Quadt,[22] B. Quinn,[64] K.J. Rani,[29] K. Ranjan,[28] P.A. Rapidis,[49] P.N. Ratoff,[41] S. Reucroft,[61] M. Rijssenbeek,[69] I. Ripp-Baudot,[19] F. Rizatdinova,[57] S. Robinson,[42] R.F. Rodrigues,[3] C. Royon,[18] P. Rubinov,[49] R. Ruchti,[54] V.I. Rud,[37] G. Sajot,[14] A. Sánchez-Hernández,[32] M.P. Sanders,[59] A. Santoro,[3] G. Savage,[49] L. Sawyer,[58] T. Scanlon,[42] D. Schaile,[25] R.D. Schamberger,[69] H. Schellman,[52] P. Schieferdecker,[25] C. Schmitt,[26] C. Schwanenberger,[22] A. Schwartzman,[66] R. Schwienhorst,[63] S. Sengupta,[48] H. Severini,[72] E. Shabalina,[50] M. Shamim,[57] V. Shary,[18] A.A. Shchukin,[38] W.D. Shephard,[54] R.K. Shivpuri,[28] D. Shpakov,[61] R.A. Sidwell,[57] V. Simak,[10] V. Sirotenko,[49] P. Skubic,[72] P. Slattery,[68] R.P. Smith,[49] K. Smolek,[10] G.R. Snow,[65] J. Snow,[71] S. Snyder,[70] S. Söldner-Rembold,[43] X. Song,[51] L. Sonnenschein,[17] A. Sopczak,[41] M. Sosebee,[74] K. Soustruznik,[9] M. Souza,[2] B. Spurlock,[74] N.R. Stanton,[57] J. Stark,[14] J. Steele,[58] K. Stevenson,[53] V. Stolin,[36] A. Stone,[50] D.A. Stoyanova,[38] J. Strandberg,[40] M.A. Strang,[74] M. Strauss,[72] R. Ströhmer,[25] D. Strom,[52] M. Strovink,[45] L. Stutte,[49] S. Sumowidagdo,[48] A. Sznajder,[3] M. Talby,[15] P. Tamburello,[44] W. Taylor,[5] P. Telford,[43] J. Temple,[44] M. Tomoto,[49] T. Toole,[59] J. Torborg,[54] S. Towers,[69] T. Trefzger,[24] S. Trincaz-Duvoid,[17] B. Tuchming,[18] C. Tully,[66] A.S. Turcot,[43] P.M. Tuts,[67] L. Uvarov,[39] S. Uvarov,[39] S. Uzunyan,[51] B. Vachon,[5] R. Van Kooten,[53] W.M. van Leeuwen,[33] N. Varelas,[50] E.W. Varnes,[44] A. Vartapetian,[74] I.A. Vasilyev,[38] M. Vaupel,[26] P. Verdier,[20] L.S. Vertogradov,[35] M. Verzocchi,[59] F. Villeneuve-Seguier,[42] J.-R. Vlimant,[17] E. Von Toerne,[57] M. Vreeswijk,[33] T. Vu Anh,[16] H.D. Wahl,[48] L. Wang,[59] J. Warchol,[54] G. Watts,[78] M. Wayne,[54] M. Weber,[49] H. Weerts,[63] M. Wegner,[21] N. Wermes,[22] A. White,[74] V. White,[49] D. Wicke,[49] D.A. Wijngaarden,[34] G.W. Wilson,[56] S.J. Wimpenny,[47] J. Wittlin,[60] M. Wobisch,[49] J. Womersley,[49] D.R. Wood,[61] T.R. Wyatt,[43] Q. Xu,[62] N. Xuan,[54] S. Yacoob,[52] R. Yamada,[49] M. Yan,[59] T. Yasuda,[49] Y.A. Yatsunenko,[35] Y. Yen,[26] K. Yip,[70] H.D. Yoo,[73] S.W. Youn,[52] J. Yu,[74] A. Yurkewicz,[69] A. Zabi,[16] A. Zatserklyaniy,[51] M. Zdrazil,[69] C. Zeitnitz,[24] D. Zhang,[49] X. Zhang,[72] T. Zhao,[78] Z. Zhao,[62] B. Zhou,[62] J. Zhu,[69] M. Zielinski,[68] D. Zieminska,[53] A. Zieminski,[53] R. Zitoun,[69] V. Zutshi,[51] and E.G. Zverev[37]
(DØ Collaboration)

[1] *Universidad de Buenos Aires, Buenos Aires, Argentina*
[2] *LAFEX, Centro Brasileiro de Pesquisas Físicas, Rio de Janeiro, Brazil*
[3] *Universidade do Estado do Rio de Janeiro, Rio de Janeiro, Brazil*
[4] *Instituto de Física Teórica, Universidade Estadual Paulista, São Paulo, Brazil*
[5] *University of Alberta, Edmonton, Alberta, Canada, Simon Fraser University, Burnaby, British Columbia, Canada, York University, Toronto, Ontario, Canada, and McGill University, Montreal, Quebec, Canada*
[6] *Institute of High Energy Physics, Beijing, People's Republic of China*
[7] *University of Science and Technology of China, Hefei, People's Republic of China*
[8] *Universidad de los Andes, Bogotá, Colombia*
[9] *Center for Particle Physics, Charles University, Prague, Czech Republic*
[10] *Czech Technical University, Prague, Czech Republic*
[11] *Institute of Physics, Academy of Sciences, Center for Particle Physics, Prague, Czech Republic*
[12] *Universidad San Francisco de Quito, Quito, Ecuador*
[13] *Laboratoire de Physique Corpusculaire, IN2P3-CNRS, Université Blaise Pascal, Clermont-Ferrand, France*
[14] *Laboratoire de Physique Subatomique et de Cosmologie, IN2P3-CNRS, Universite de Grenoble 1, Grenoble, France*
[15] *CPPM, IN2P3-CNRS, Université de la Méditerranée, Marseille, France*
[16] *Laboratoire de l'Accélérateur Linéaire, IN2P3-CNRS, Orsay, France*
[17] *LPNHE, IN2P3-CNRS, Universités Paris VI and VII, Paris, France*
[18] *DAPNIA/Service de Physique des Particules, CEA, Saclay, France*
[19] *IReS, IN2P3-CNRS, Université Louis Pasteur, Strasbourg, France, and Université de Haute Alsace, Mulhouse, France*
[20] *Institut de Physique Nucléaire de Lyon, IN2P3-CNRS, Université Claude Bernard, Villeurbanne, France*
[21] *III. Physikalisches Institut A, RWTH Aachen, Aachen, Germany*
[22] *Physikalisches Institut, Universität Bonn, Bonn, Germany*
[23] *Physikalisches Institut, Universität Freiburg, Freiburg, Germany*
[24] *Institut für Physik, Universität Mainz, Mainz, Germany*
[25] *Ludwig-Maximilians-Universität München, München, Germany*
[26] *Fachbereich Physik, University of Wuppertal, Wuppertal, Germany*
[27] *Panjab University, Chandigarh, India*
[28] *Delhi University, Delhi, India*
[29] *Tata Institute of Fundamental Research, Mumbai, India*
[30] *University College Dublin, Dublin, Ireland*

[31] *Korea Detector Laboratory, Korea University, Seoul, Korea*
[32] *CINVESTAV, Mexico City, Mexico*
[33] *FOM-Institute NIKHEF and University of Amsterdam/NIKHEF, Amsterdam, The Netherlands*
[34] *Radboud University Nijmegen/NIKHEF, Nijmegen, The Netherlands*
[35] *Joint Institute for Nuclear Research, Dubna, Russia*
[36] *Institute for Theoretical and Experimental Physics, Moscow, Russia*
[37] *Moscow State University, Moscow, Russia*
[38] *Institute for High Energy Physics, Protvino, Russia*
[39] *Petersburg Nuclear Physics Institute, St. Petersburg, Russia*
[40] *Lund University, Lund, Sweden, Royal Institute of Technology and Stockholm University, Stockholm, Sweden, and Uppsala University, Uppsala, Sweden*
[41] *Lancaster University, Lancaster, United Kingdom*
[42] *Imperial College, London, United Kingdom*
[43] *University of Manchester, Manchester, United Kingdom*
[44] *University of Arizona, Tucson, Arizona 85721, USA*
[45] *Lawrence Berkeley National Laboratory and University of California, Berkeley, California 94720, USA*
[46] *California State University, Fresno, California 93740, USA*
[47] *University of California, Riverside, California 92521, USA*
[48] *Florida State University, Tallahassee, Florida 32306, USA*
[49] *Fermi National Accelerator Laboratory, Batavia, Illinois 60510, USA*
[50] *University of Illinois at Chicago, Chicago, Illinois 60607, USA*
[51] *Northern Illinois University, DeKalb, Illinois 60115, USA*
[52] *Northwestern University, Evanston, Illinois 60208, USA*
[53] *Indiana University, Bloomington, Indiana 47405, USA*
[54] *University of Notre Dame, Notre Dame, Indiana 46556, USA*
[55] *Iowa State University, Ames, Iowa 50011, USA*
[56] *University of Kansas, Lawrence, Kansas 66045, USA*
[57] *Kansas State University, Manhattan, Kansas 66506, USA*
[58] *Louisiana Tech University, Ruston, Louisiana 71272, USA*
[59] *University of Maryland, College Park, Maryland 20742, USA*
[60] *Boston University, Boston, Massachusetts 02215, USA*
[61] *Northeastern University, Boston, Massachusetts 02115, USA*
[62] *University of Michigan, Ann Arbor, Michigan 48109, USA*
[63] *Michigan State University, East Lansing, Michigan 48824, USA*
[64] *University of Mississippi, University, Mississippi 38677, USA*
[65] *University of Nebraska, Lincoln, Nebraska 68588, USA*
[66] *Princeton University, Princeton, New Jersey 08544, USA*
[67] *Columbia University, New York, New York 10027, USA*
[68] *University of Rochester, Rochester, New York 14627, USA*
[69] *State University of New York, Stony Brook, New York 11794, USA*
[70] *Brookhaven National Laboratory, Upton, New York 11973, USA*
[71] *Langston University, Langston, Oklahoma 73050, USA*
[72] *University of Oklahoma, Norman, Oklahoma 73019, USA*
[73] *Brown University, Providence, Rhode Island 02912, USA*
[74] *University of Texas, Arlington, Texas 76019, USA*
[75] *Southern Methodist University, Dallas, Texas 75275, USA*
[76] *Rice University, Houston, Texas 77005, USA*
[77] *University of Virginia, Charlottesville, Virginia 22901, USA*
[78] *University of Washington, Seattle, Washington 98195, USA*

(Dated: April 28, 2005)

We present a measurement of the top quark pair ($t\bar{t}$) production cross section ($\sigma_{t\bar{t}}$) in $p\bar{p}$ collisions at $\sqrt{s} = 1.96$ TeV using 230 pb^{-1} of data collected by the DØ experiment at the Fermilab Tevatron Collider. We select events with one charged lepton (electron or muon), missing transverse energy, and jets in the final state. We employ lifetime-based b-jet identification techniques to further enhance the $t\bar{t}$ purity of the selected sample. For a top quark mass of 175 GeV, we measure $\sigma_{t\bar{t}} = 8.6^{+1.6}_{-1.5}$ (stat. + syst.) $\pm$ 0.6 (lumi.) pb, in agreement with the standard model expectation.

PACS numbers: 13.85.Lg, 13.85.Qk, 14.65.Ha

The top quark was discovered at the Fermilab Tevatron Collider by the CDF and DØ collaborations [1] in $p\bar{p}$ collisions at $\sqrt{s} = 1.8$ TeV based on about 50 pb^{-1} of data per experiment. The increased statistics and higher collision energy of $\sqrt{s} = 1.96$ TeV of Tevatron Run II allow more precise measurements of top quark properties, including its production and decay characteristics. Theoretical calculations performed within the framework of the standard model (SM) predict the $t\bar{t}$ production cross section ($\sigma_{t\bar{t}}$) with an uncertainty of less than 15% [2]. A significant deviation from this prediction would signal the presence of physics beyond the SM, such as $t\bar{t}$ resonant production [3]. The CDF and DØ collaborations have previously reported measurements of $\sigma_{t\bar{t}}$ at $\sqrt{s} = 1.8$ TeV [4]. Recent measurements at $\sqrt{s} = 1.96$ TeV by the CDF [5] and DØ [6] collaborations agree with the SM prediction within their experimental uncertainties.

In the SM, the top quark decays to a W boson and b quark with a branching ratio of $\approx 100\%$. The lepton+jets final state results from the leptonic decay of one of the W bosons and the hadronic decay of the other. The event signature is one lepton with high transverse momentum, large transverse energy imbalance ($\not\!\!E_T$) due to the undetected neutrino, and four jets, two of which result from hadronization of the b quarks.

In this Letter, we report the measurement of $\sigma_{t\bar{t}}$ in the lepton (electron or muon) plus jets channel using b-jet identification (b-tagging) techniques exploiting the long lifetime of B hadrons. The data were collected by the DØ experiment from August 2002 through March 2004, and correspond to an integrated luminosity of 226 ± 15 pb^{-1} (229 ± 15 pb^{-1}) in the electron (muon) sample.

The DØ detector includes a tracking system, calorimeters, and a muon spectrometer [7]. The tracking system consists of a silicon microstrip tracker (SMT) and a central fiber tracker (CFT), both located inside a 2 T superconducting solenoid. The tracker design provides efficient charged particle measurements in the pseudorapidity region $|\eta| < 3$ [8]. The SMT strip pitch of 50–80 μm allows a precise reconstruction of the primary interaction vertex (PV) and an accurate determination of the impact parameter of a track relative to the PV [9], which are the key components of the lifetime-based b-jet tagging algorithms. The PV is required to be within the SMT fiducial volume and consist of at least 3 tracks. The calorimeter consists of a central section (CC) covering $|\eta| < 1.1$, and two end calorimeters (EC) extending the coverage to $|\eta| \approx 4.2$. The muon system surrounds the calorimeter and consists of three layers of tracking detectors and two layers of scintillators [10]. A 1.8 T iron toroidal magnet is located outside the innermost layer of the muon detector. The luminosity is calculated from the rate for $p\bar{p}$ inelastic collisions detected using two hodoscopes of scintillation counters mounted close to the beam pipe on the front surfaces of the EC calorimeters.

We select data samples in the electron and muon channels by requiring an isolated electron with $p_T > 20$ GeV and $|\eta| < 1.1$, or an isolated muon with $p_T > 20$ GeV and $|\eta| < 2.0$. More details on the lepton identification as well as trigger requirements are reported elsewhere [6]. In both channels, we require $\not\!\!E_T$ to exceed 20 GeV and not be collinear with the lepton direction in the transverse plane. These W boson candidate events must be accompanied by one or more jets with $p_T > 15$ GeV and rapidity $|y| < 2.5$ [8]. Jets are defined using a cone algorithm with radius $\Delta\mathcal{R} = 0.5$ [11]. We classify the selected events according to their jet multiplicity. Events with 3 or ≥ 4 jets are expected to be enriched in $t\bar{t}$ signal, whereas events with only 1 or 2 jets are expected to be dominated by background. We use the former to estimate $\sigma_{t\bar{t}}$, and the latter to verify the background normalization procedure.

The main background in this analysis is the production of W bosons in association with jets (W+jets), with the W boson decaying leptonically. In most cases, the jets accompanying the W boson originate from light (u, d, s) quarks and gluons (W+light jets). Depending on the jet multiplicity, between 2% and 14% of W+jets events contain heavy flavor jets resulting from gluon splitting into $b\bar{b}$ or $c\bar{c}$ ($Wb\bar{b}$ or $Wc\bar{c}$, respectively), while in about 5% of events, a single c quark is present in the final state as a result of the W boson radiated from an s quark from the proton's or antiproton's sea (Wc). A sizeable background arises from strong production of two or more jets ("multijets"), with one of the jets misidentified as a lepton and accompanied by large $\not\!\!E_T$ resulting from mismeasurements of jet energies. Significantly smaller contributions to the background arise from single top, Z+jets, and weak diboson (WW, WZ and ZZ) production. Only a small fraction of the background events contain b or c-quark jets in the final state. As a consequence, the signal-to-background ratio is significantly enhanced when at least one jet is identified as a b-quark jet.

We use a secondary vertex tagging (SVT) algorithm to identify b-quark jets. Secondary vertices are reconstructed from two or more tracks satisfying the following requirements: $p_T > 1$ GeV, ≥ 1 hits in the SMT layers and impact parameter significance $d_{ca}/\sigma_{d_{ca}} > 3.5$ [9]. Tracks identified as arising from K^0_S or Λ decays or from γ conversions are not considered. If the secondary vertex reconstructed within a jet has a decay length significance $L_{xy}/\sigma_{L_{xy}} > 7$ [12], the jet is tagged as a b-quark jet. Events with exactly 1 (≥ 2) tagged jets are referred to as single-tag (double-tag) events. We treat single-tag and double-tag events separately because of their different signal-to-background ratios.

Secondary vertices with $L_{xy}/\sigma_{L_{xy}} < -7$ appear due to finite resolution of their characteristics after reconstruction, and define the "negative tagging rate". The negative tagging rate is used to estimate the probability for misidentifying a light flavor (u, d, s quark or gluon) jet as a b-quark jet (the "mis-tagging rate").

We estimate both the b-tagging efficiency and the mistagging rate using jets with ≥ 2 tracks satisfying less stringent requirements than those for SVT. In particular,

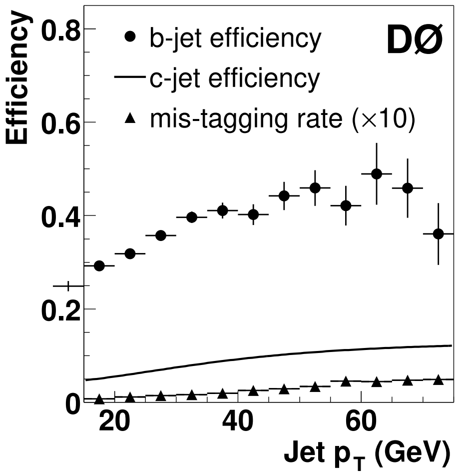

FIG. 1: Measured b-tagging efficiency (circles) and mis-tagging rate (triangles), and estimated c-tagging efficiency (solid line) as a function of jet p_T.

the p_T cut is reduced from 1 GeV to 0.5 GeV for all but the highest p_T track, and no cut on $d_{ca}/\sigma_{d_{ca}}$ of the tracks is made. These requirements have an efficiency per jet > 80% for $p_T > 30$ GeV and integrated over y. We measure the b-tagging efficiency in a data sample of dijet events with enhanced heavy flavor content by requiring a jet with an associated muon at high transverse momentum relative to the jet axis. By comparing the SVT and muon-tagged jet samples, the tagging efficiency for semileptonic b-quark decays ("semileptonic b-tagging efficiency") can be inferred. We make use of a Monte Carlo (MC) simulation to further correct the measured efficiency to the tagging efficiency for inclusive b-quark decays. We estimate the c-tagging efficiency from the same simulation, corrected by a scale factor defined as the ratio of the semileptonic b-tagging efficiency measured in data to that measured in the simulation. We estimate the mis-tagging rate from the negative tagging rate measured in dijet events, corrected for the contribution of heavy-flavor jets and the presence of long-lived particles in light-flavor jets. Figure 1 shows the b-tagging efficiency, c-tagging efficiency and mis-tagging rate as a function of jet p_T.

We simulate $t\bar{t}$ production, and all background processes except multijets, using ALPGEN [13] to generate the parton-level processes, and PYTHIA [14] to provide fragmentation and to decay all unstable particles except B hadrons and τ leptons, which are modeled via EVTGEN [15] and TAUOLA [16], respectively. We process the generated events through the full GEANT-based [17] DØ detector simulation and the same reconstruction program used to process the data. We apply small additional smearing to the reconstructed objects to improve the agreement between the data and the simulation, and account for remaining discrepancies using correction factors derived by comparing the efficiencies measured in $Z \to \ell^+\ell^-$ data to those obtained from the simulation. For all processes except the multijets background, we make use of the MC simulation to compute the total acceptance, applying the trigger, reconstruction and tagging efficiencies measured using data. The tagging probability for a particular process depends on the flavor composition of the jets in the final state as well as on the overall event kinematics. We estimate it by applying the tagging rates measured in data to each jet in the simulation, taking into consideration its flavor, p_T, and y. In the case of W+jets events, we also use the simulation to estimate the fraction of the different W+heavy flavor subprocesses.

We compute the $t\bar{t}$ acceptance for events with a true electron or muon arising from a $W \to \ell\nu$ ($\ell = e, \mu, \tau$) decay, corresponding to total branching fractions of 17.106% and 17.036% [18], respectively, in the electron and muon channels. In the electron channel, the total acceptance before tagging is estimated to be (10.8 ± 0.8)% and (14.2 ± 1.7)%, for events with 3 and those with ≥ 4 jets, respectively. The corresponding numbers for the muon channel are (9.9 ± 1.0)% and (14.1 ± 1.9)%. The estimated single-tag efficiencies are (43.4 ± 1.2)% and (45.3 ± 1.0)% for events with 3 and those with ≥ 4 jets, respectively. The corresponding double-tag efficiencies are (10.4 ± 1.0)% and (14.2 ± 1.3)%.

We estimate the number of multijet events from the data for each jet multiplicity using the matrix method described in Ref. [6], separately for the samples before and after tagging. Smaller contributions from single top, Z+jets, and diboson production (collectively referred to as "other bkg") are estimated from the simulation, normalized to the next-to-leading order theoretical cross sections [19, 20]. We also include under "other bkg" the contribution from $t\bar{t}$ with both W bosons decaying leptonically, assuming the same $\sigma_{t\bar{t}}$ as for $t\bar{t} \to \ell$+jets. We determine the number of tagged W+jets events as the product of the number of W+jets events in data before tagging and the average tagging probability for W+jets events (e.g. ≈ 4% for single-tag and ≈ 0.4% for double-tag events with ≥ 4 jets). The number of W+jets events before tagging is computed as a difference between the number of selected events and the estimated contribution from the rest of processes (multijets, $t\bar{t}$, and "other bkg").

Tables I and II summarize the sample composition for single-tag and double-tag events, respectively, assuming $\sigma_{t\bar{t}} = 7.0$ pb. Figure 2 shows the observed and expected number of events for each jet multiplicity. We interpret the excess over the background expectation in the third and fourth jet multiplicity bins as the $t\bar{t}$ signal. The good agreement between observation and expectation in the first and second jet multiplicity bins validates the background estimation procedure.

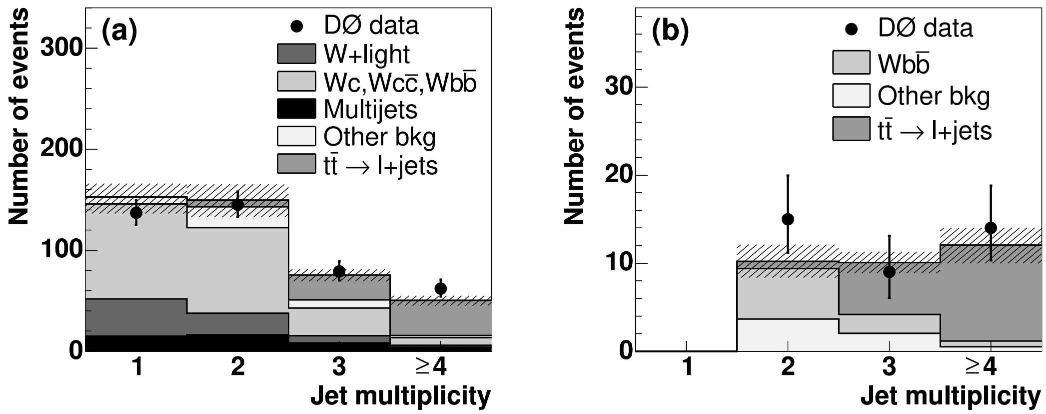

FIG. 2: Expected and observed number of (a) single-tag and (b) double-tag events. The hatched area represents the total uncertainty in the expectation.

TABLE I: Summary of observed and expected numbers of events before tagging and with exactly one jet tagged.

	$W+1$ jet	$W+2$ jets	$W+3$ jets	$W+\geq 4$ jets
		Before tagging		
Observed	14054	5502	1365	367
Multijets	718±78	516±43	190±14	66±6
		After tagging		
W+light	36.8±4.0	21.4±2.4	7.2±0.9	1.8±0.3
Wc	47.8±5.4	24.2±2.7	5.7±0.7	0.8±0.1
$Wc\bar{c}$	12.2±3.4	17.2±4.8	6.6±1.9	2.2±0.7
$Wb\bar{b}$	33.9±8.7	43.2±11.0	15.1±3.9	4.5±1.3
Multijets	14.9±1.9	16.3±2.1	8.3±1.5	4.0±1.2
Other bkg	6.6±0.9	20.6±2.1	8.2±0.8	2.2±0.4
Total bkg	152.4±14.8	142.9±16.0	51.0±5.6	15.6±1.7
$t\bar{t} \to \ell$+jets	0.4±0.1	6.8±1.4	24.4±1.7	34.8±4.3
Total expected	152.8±14.8	149.7±16.2	75.4±5.9	50.4±4.8
Observed	137	145	79	62

TABLE II: Summary of observed and expected number of events with two or more jets tagged.

	W+2jets	W+3jets	$W+\geq$4jets
$Wb\bar{b}$	5.7±1.6	2.2±0.6	0.7±0.2
Other bkg	3.7±0.4	2.0±0.3	0.5±0.3
Total bkg	9.4±1.8	4.2±0.8	1.2±0.3
$t\bar{t} \to \ell$+jets	0.8±0.2	5.9±0.7	10.9±1.9
Total expected	10.2±1.9	10.1±1.2	12.1±2.0
Observed	15	9	14

We calculate $\sigma_{t\bar{t}}$ by maximizing a likelihood function including a Poisson term for each of the eight independent channels considered: 3 and $\geq$ 4 jets, for single- and double-tag events in the electron and muon channels. At each step in the maximization, the multijet background in these eight tagged samples, and the corresponding samples before tagging, is constrained within errors to the amount determined by the matrix method. In addition, we include a Gaussian term for each of the systematic uncertainties considered, following the procedure described in Ref. [21]. In this approach, each source of systematic uncertainty is allowed to affect the central value of the cross section during the maximization procedure, thus yielding a combined statistical and systematic uncertainty on $\sigma_{t\bar{t}}$. Assuming a top quark mass (m_t) of 175 GeV, we measure

$$\sigma_{t\bar{t}} = 8.6^{+1.6}_{-1.5}\,(\text{stat.} + \text{syst.}) \pm 0.6\,(\text{lumi.})\ \text{pb},$$

in good agreement with the SM prediction of 6.77 ± 0.42 pb [2].

The contribution due to each individual source of systematic uncertainty can be estimated by redoing the fit after fixing all but the corresponding Gaussian term and unfolding the statistical uncertainty from the resulting total uncertainty. The statistical uncertainty of $^{+1.2}_{-1.1}$ pb is obtained from the fit where all Gaussian terms are fixed. As shown in Table III, b-jet tagging efficiency, jet energy calibration, and background modeling are the leading sources of systematic uncertainty. In addition, a systematic uncertainty of 6.5% from the luminosity measurement [22] has been assigned. In the top quark mass

TABLE III: Summary of systematic uncertainties on $\sigma_{t\bar{t}}$.

Source	$\Delta\sigma_{t\bar{t}}$ (pb)
b-tagging efficiency	+0.6 − 0.5
Jet energy calibration	+0.5 − 0.4
Background modeling	±0.5
Lepton selections	+0.5 − 0.4
Jet identification	+0.3 − 0.2
Multijet background	+0.3 − 0.2
Mis-tagging rate	±0.1
Total	+1.1 − 1.0

range of 160 GeV to 190 GeV, the measured cross section decreases (increases) by 0.06 pb per 1 GeV shift of m_t above (below) 175 GeV.

We used an alternative b-tagging algorithm to cross check this result. This algorithm relies on counting tracks with significant impact parameter (CSIP) with respect to the PV: a jet is tagged if ≥ 2 (≥ 3) associated tracks have $d_{ca}/\sigma_{d_{ca}} > 3$ ($d_{ca}/\sigma_{d_{ca}} > 2$). As compared to SVT, this algorithm has a slightly higher b-tagging efficiency and about a factor of two higher mis-tagging rate. The measured cross section using the CSIP algorithm is $\sigma_{t\bar{t}} = 7.6^{+1.7}_{-1.4}$ (stat. + syst.) $\pm$ 0.5 (lumi.) pb, consistent with the SVT result once the existing overlap between both samples is taken into account. While we are currently not combining these two results, the fact that different b-tagging techniques are only partially correlated will be exploited in future analyses to further increase the precision of this measurement.

In summary, we have measured the $t\bar{t}$ production cross section in $p\bar{p}$ interactions at $\sqrt{s} = 1.96$ TeV in the lepton+jets channel using lifetime b-tagging. Our measurement yields $\sigma_{t\bar{t}} = 8.6^{+1.6}_{-1.5}$ (stat. + syst.) $\pm$ 0.6 (lumi.) pb, in a good agreement with the SM prediction.

We thank the staffs at Fermilab and collaborating institutions, and acknowledge support from the DOE and NSF (USA), CEA and CNRS/IN2P3 (France), FASI, Rosatom and RFBR (Russia), CAPES, CNPq, FAPERJ, FAPESP and FUNDUNESP (Brazil), DAE and DST (India), Colciencias (Colombia), CONACyT (Mexico), KRF (Korea), CONICET and UBACyT (Argentina), FOM (The Netherlands), PPARC (United Kingdom), MSMT (Czech Republic), CRC Program, CFI, NSERC and WestGrid Project (Canada), BMBF and DFG (Germany), SFI (Ireland), A.P. Sloan Foundation, Research Corporation, Texas Advanced Research Program, Alexander von Humboldt Foundation, and the Marie Curie Fellowships.

[*] Visitor from University of Zurich, Zurich, Switzerland.

[1] CDF Collaboration, F. Abe *et al.*, Phys. Rev. Lett. **74**, 2626 (1995); DØ Collaboration, S. Abachi *et al.*, Phys. Rev. Lett. **74**, 2632 (1995).

[2] R. Bonciani *et al.*, Nucl. Phys. B **529**, 424 (1998); M. Cacciari *et al.*, JHEP **0404**, 068 (2004); N. Kidonakis and R. Vogt, Phys. Rev. D **68**, 114014 (2003).

[3] C. T. Hill and S. J. Parke, Phys. Rev. D **49**, 4454 (1994); H. P. Nilles, Phys. Rep. **110**, 1 (1984); H. E. Haber and G. L. Kane, *ibid.* **117**, 75 (1985).

[4] CDF Collaboration, T. Affolder *et al.*, Phys. Rev. D **64**, 032002 (2001); DØ Collaboration, V. Abazov *et al.*, Phys. Rev. D **67**, 012004 (2003).

[5] CDF Collaboration, D. Acosta *et al.*, Phys. Rev. Lett. **93**, 142001 (2004); CDF Collaboration, D. Acosta *et al.*, Phys. Rev. D **71**, 072005 (2005); CDF Collaboration, D. Acosta *et al.*, Phys. Rev. D **71**, 052003 (2005).

[6] DØ Collaboration, V. Abazov *et al.*, hep-ex/0504043.

[7] DØ Collaboration, V. Abazov *et al.*, "The Upgraded DØ Detector", in preparation for submission to Nucl. Instrum. Methods Phys. Res. A.

[8] Rapidity y and pseudorapidity η are defined as functions of the polar angle θ and parameter β as $y(\theta, \beta) \equiv \frac{1}{2} \ln [(1 + \beta \cos\theta)/(1 - \beta \cos\theta)]$ and $\eta(\theta) \equiv y(\theta, 1)$, where β is the ratio of a particle's momentum to its energy.

[9] Impact parameter is defined as the distance of closest approach (d_{ca}) of the track to the primary vertex in the plane transverse to the beamline. Impact parameter significance is defined as $d_{ca}/\sigma_{d_{ca}}$, where $\sigma_{d_{ca}}$ is the uncertainty on d_{ca}.

[10] V. Abazov *et al.*, FERMILAB-PUB-05-034-E (2005).

[11] We use the iterative, seed-based cone algorithm including midpoints, as described on p. 47 in G. C. Blazey *et al.* , in Proceedings of the Workshop: *"QCD and Weak Boson Physics in Run II",* edited by U. Baur, R. K. Ellis, and D. Zeppenfeld, FERMILAB-PUB-00-297 (2000).

[12] Decay length L_{xy} is defined as the distance from the primary to the secondary vertex in the plane transverse to the beamline. Decay length significance is defined as $L_{xy}/\sigma_{L_{xy}}$, where $\sigma_{L_{xy}}$ is the uncertainty on L_{xy}.

[13] M. L. Mangano *et al.*, JHEP **07**, 001 (2003).

[14] T. Sjöstrand *et al.*, Comput. Phys. Commun. **135**, 238 (2001).

[15] D. Lange, Nucl. Instrum. Methods Phys. Res. A **462**, 152 (2001).

[16] S. Jadach *et al.*, Comp. Phys. Commun. **76**, 361 (1993).

[17] R. Brun and F. Carminati, CERN Programming Library Long Writeup **W5013** (1993).

[18] S. Eidelman *et al.*, Phys. Lett. B **592**, 1 (2004).

[19] M. C. Smith and S. Willenbrock, Phys. Rev. D **54**, 6696 (1996); T. Stelzer *et al.*, Phys. Rev. D **56**, 5919 (1997).

[20] J. M. Campbell and R. K. Ellis, Phys. Rev. D **60**, 113006 (1999).

[21] P. Sinervo, in *Proceedings of Statistical methods in Particle Physics, Astrophysics, and Cosmology*, edited by L. Lyons, R. P. Mount, and R. Reitmeyer (SLAC, Stanford, 2003), p. 334.

[22] T. Edwards *et al.*, FERMILAB-TM-2278-E (2004).